

# Determining the grain geometry from ultrasonic measurements of large-grained temperate ice cores

Jerome Graves<sup>1</sup>, Ben Lisman<sup>2</sup>, Sevan Harput<sup>3</sup>

Division of Electrical and Electronic Engineering, London South Bank University, London, U.K.

E-mail: gravesj2@lsbu.ac.uk

**Abstract**— Ice shelf collapse significantly contributes to the global rise of sea levels. This intricate process of fracturing, though not yet fully understood, is intertwined with the mechanical attributes of ice. Among the critical physical attributes related to its mechanical characteristics is the crystal orientation fabric (COF), which encapsulates the dimensions, orientations, and inclinations of the constituent crystal grains within the ice structure. The acquisition of such granular information necessitates the extraction of ice cores from the ice sheets or shelves, followed by their transportation to a controlled laboratory environment. After this, these cores are sectioned into sub-millimetre slices and examined using polarised light microscopy (PLM). However, this procedure destroys the ice core specimens and only permits the acquisition of two-dimensional images, imparting only a partial depiction of the three-dimensional COF.

The principal objective of this work is to explore the possibility of involving ultrasound technology to discern the crystal grains' COF and their geometries. This novel approach does not harm the sample material during the examination.

**Keywords**—Ice; Ultrasonics; Anisotrop; Non-destructive testing.

## I. INTRODUCTION

The structure of glacial ice is polycrystalline, with diverse configurations of crystal orientation fabric (COF) contingent upon the particular mode of its formation. These configurations are grounded in naturally occurring structures [1, 2]. The emergence of distinct COF types is based on environmental determinants, including but not limited to temperature, ice flow, impurity content, and pressure conditions [2-4]. The ice sheets are formed through the process of condensation and snow accumulation. The resultant powdery ice initially assumes a state of loose compaction characterised by randomly oriented crystals. Over time this loosely arranged structure changes into firn ice, a transitional phase between surface ice and glacial ice, distinguished by a notable air content. As geological pressures persistently exert themselves and successive compaction ensues, a recrystallisation process commences. This recrystallisation enlarges the crystal grains, and these preferential orientations emerge [2]. The porosity is reduced, the grain size is increased, and the grains are reoriented with mechanical stress and strain. Firn ice can be modelled as mechanically isotropic due to its small, randomly oriented crystals. However, with the recrystallisation process into larger grain structures, the isotropic nature transforms to mechanical anisotropy, affecting how and when fractures form with changes in atmospheric temperature [5]. Glen's flow law is the basis for most past analyses of ice sheets and glacial flow analyses. However, it does not consider the anisotropic properties of ice. More recently, the anisotropic properties of ice have been incorporated into ice flow models [6, 7].

Characterising the ice COF will allow improved parameterisation of these anisotropic flow models [8].

Ice is transversely anisotropic. Its structure has symmetry along one axis; the other two are asymmetrical. This causes the acoustic properties (impedance and velocity) to vary depending on the crystal's inclination and orientation.

The anisotropy of ice can lead to changes in the velocity and amplitude of ultrasonic waves, depending on the orientation of the ice crystals relative to the ultrasound probe [9] when ultrasonic waves propagate through the ice.

## II. PROBLEM STATEMENT

Figure 1 presents an illustrative depiction of the microstructural characteristics of grains within the deep ice sheet. Specifically, the COF of an ice core extracted from the Rhonegletcher region in the Central Swiss Alps and is situated at a depth of 79 meters. The ice core in question possesses an approximate diameter of 70 mm. Notably, the predominant alignment of its grains is vertical, with other orientations aligned along the trajectory of glacial flow, measuring 155°. Visualising grain geometry through ultrasonic measurements requires discernible differences in acoustic impedance between grains of different orientations and inclinations.



Fig. 1. COF of an ice core from Rhonegletcher, Central Swiss Alps, at a depth of 79m. The diameter is approximately 70mm.

## III. METHODS

### A. Simulations

The initial verification was performed using the MTeX simulation toolbox in MATLAB. We assume near-perfect hexagonal ice ( $I^h$ ) with no impurities. The seismic anisotropy of ice can be described as a fourth-order elasticity tensor. Due to the symmetry of ice ( $I^h$ ), eighty-one unknown elements can be reduced to five constraints for a monocrystal [10]. We use the elasticity tensor calculated from Benet at  $T = -10^\circ\text{C}$ , which has provided the best agreement between calculated and measured data in previous ultrasonic experiments [9]. The elasticity

tensor, crystal shape and symmetry values derive the ultrasonic velocity of ice at all orientations and inclinations using the Christoffel equation [11-14].

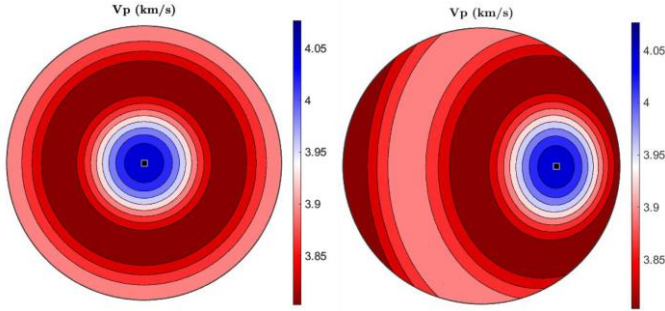


Fig. 2. Upper-hemisphere plots of the p-wave velocity of an ice monocrystal. (Left) orientation (0,0,0). (right) orientation (45,0,0).

## B. Experiments

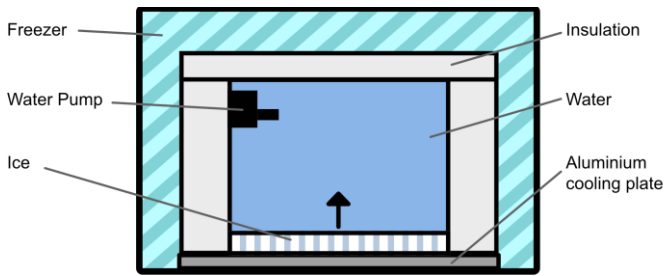


Fig. 3. Apparatus for growing ice using the directional freezing technique.

Fig 3 shows the apparatus that was made to create ice samples. The mixture of the bottom-up freezing technique and agitation of the surface water gives a polycrystalline structure of mostly vertical grains with no dendritic growth and no air bubbles [3, 15]. They were frozen at  $-10^{\circ}\text{C}$  to encourage larger crystal formation. The grain size varies from 5-20 mm (Fig 4). A band saw is used to cut this ice into pieces across the z-axis at different angles modifying the average inclination of grains to:  $(0^{\circ}, 20^{\circ}, 45^{\circ})$ . They were then machined into cylinders with a diameter of 100mm and height of 25mm, using a 3-axis CNC router. The orientation of the inclination was marked on each sample.

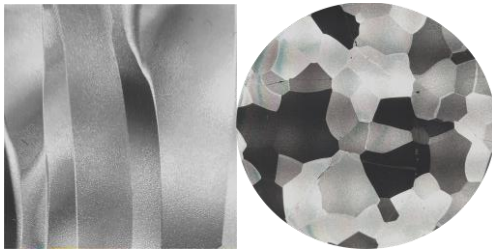


Fig. 4. (Left) PLM photo of  $0^{\circ}$  ice sample in vertical plane. (Right) PLM photos of  $0^{\circ}$  ice sample in the horizontal plane

The experimental setup (Fig 5) consisted of two 6 mm diameter, submersible single-element connected to horizontal motion stages with 0.01mm accuracy. The ice was frozen to a base attached, between the transducers, to a rotational stage with a  $1^{\circ}$  accuracy. This was placed in a freezer kept at  $-10^{\circ}\text{C}$ . Glycerol was used as a couplant. The single-element transducer

was driven with a one-cycle square wave signal at 1 MHz frequency. Measurements were taken every  $10^{\circ}$  with the diameter of the core and time-of-flight of the ultrasonic wave recorded.

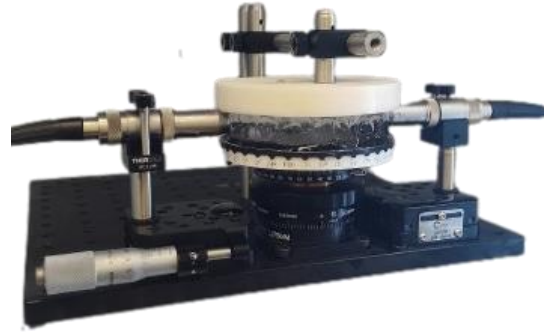


Fig. 5. Experimental setup for ultrasonic measurements.

## IV. RESULTS AND DISCUSSION

### A. Simulation

The simulation shows two maximums at  $0^{\circ}$  and  $90^{\circ}$  with a vertical ice monocrystal. The highest velocity is at  $90^{\circ}$  inclination. This is agreeable to measured values [15]. The second maximum is 3.9 km/s. The minimum velocity is 3.8 km/s at a  $45^{\circ}$  inclination.

Between monocrystal inclinations  $0^{\circ}$  and  $45^{\circ}$  the velocity variation with azimuth can be modelled as a sine wave. Its peaks are perpendicular, and troughs are parallel to the crystal's orientation. The maximum value is 3.9 km/s, and its minimum value will be between 3.8km/s and 3.9 km/s depending on the amount of inclination, with  $0^{\circ}$  at 0 km/s<sup>pk-pk</sup> and  $45^{\circ}$  at 100 km/s<sup>pk-pk</sup>.

### B. Experimental demonstration

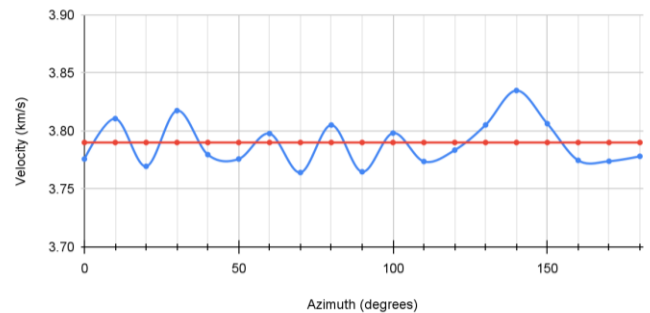


Fig. 6.  $0^{\circ}$  inclination (Blue) Measured velocity against azimuth along the isotropic plane. (Red) Average velocity across all azimuths.

Unlike the simulated monocrystalline ice, the ice samples are polycrystalline with impurities. They are grown with directional freezing to encourage vertical grains, but PLM images show slight variations in orientation and inclination. We first take reading across its isotropic axis ( $0^{\circ}$  inclination) and compare the values with the simulation. We see that the sample is isotropic along this plane but with a lower average velocity than predicted ( $\sim 0.1$  km/s, Fig. 6.). We assume that this is due to impurities in our sample and that these impurities are evenly

distributed and use this difference as an offset. It is applied to our measurements to account for impurities.

As seen in Fig. 7, when the offset is applied, we see a correlation between the simulation and measured results with a recorded minimum parallel to the orientation of the ice sample and the maximum perpendicular. The peak-to-peak value also increases with the inclination.

The variation in

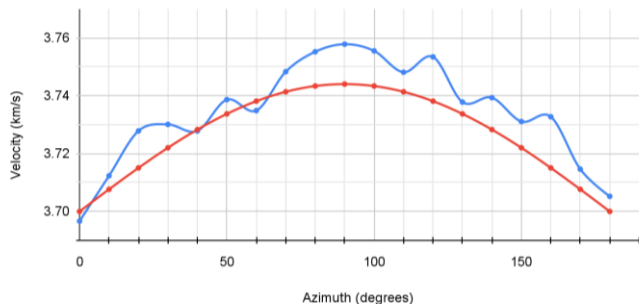


Fig. 7. 20° inclination, 90° orientation, (Blue) measured velocities, (Red) predicted velocities with offset applied.

## V. CONCLUSIONS

The specimens have slightly smaller grain sizes, ranging from 10 to 15 mm. Nonetheless, owing to the observed uniformity in their orientations and inclinations, these samples are assumed to have the same anisotropic attributes as a solitary monocrystalline ice specimen. A correlation between the ascertained measurements and the simulated ultrasound velocities becomes evident upon implementing an offset necessitated by impurities.

With deep, large-grained ice, there is a recrystallisation process that causes neighbouring grains with similar orientations and inclinations to fuse due to pressure [2]. This points to reflection data due to different ultrasound velocities and the possibility of imaging the grain geometry of large-grained ice.

## References

[1] T. M. Jordan, C. Martín, A. M. Brisbourne, D. M. Schroeder and A. M. Smith, "Radar Characterization of Ice Crystal Orientation Fabric and Anisotropic Viscosity Within an Antarctic Ice Stream," *JGR Earth Surface*, vol. 127, (6), 2022.

[2] J. H. Kennedy, E. C. Pettit and C. L. Di Prinzio, "The evolution of crystal fabric in ice sheets and its link to climate history," *Journal of Glaciology*, vol. 59, (214), pp. 357-373, 2013. Available: <https://dx.doi.org/10.3189/2013JoG12J159>.

[3] F. G. J. Perey and E. R. Pounder, "CRYSTAL ORIENTATION IN ICE SHEETS1," *Canadian Journal of Physics*, vol. 36, (4), pp. 494-502, Apr 1, 1958.

[4] T. Saruya, S. Fujita, Y. Iizuka, A. Miyamoto, H. Ohno, A. Hori, W. Shigeyama, M. Hirabayashi and K. Goto-Azuma,

"Development of crystal orientation fabric in the Dome Fuji ice core in East Antarctica: implications for the deformation regime in ice sheets," *The Cryosphere*, vol. 16, (7), pp. 2985-3003, 2022. Available:

<https://search.proquest.com/docview/2694824328>.

[5] D. G. Vaughan, "West Antarctic Ice Sheet collapse - the fall and rise of a paradigm," *Climatic Change*, vol. 91, (1-2), pp. 65-79, 2008. Available: <https://agris.fao.org/agris-search/search.do?recordID=#61:US201301552966>.

[6] F. Gillet-Chaulet, O. Gagliardini, J. Meyssonier, M. Montagnat and O. Castelnau, "A user-friendly anisotropic flow law for ice-sheet modeling," *Journal of Glaciology*, vol. 51, (172), pp. 3-14, 2005. Available: <https://dx.doi.org/10.3189/172756505781829584>.

[7] L. Placidi, R. Greve, H. Seddik and S. H. Faria, "Continuum-mechanical, Anisotropic Flow model for polar ice masses, based on an anisotropic Flow Enhancement factor," *Continuum Mech. Thermodyn*, vol. 22, (3), pp. 221-237, 2010. Available: <https://link.springer.com/article/10.1007/s00161-009-0126-0>.

[8] S. J. Marshall, "Recent advances in understanding ice sheet dynamics," *Earth and Planetary Science Letters*, vol. 240, (2), pp. 191-204, 2005. Available: <https://dx.doi.org/10.1016/j.epsl.2005.08.016>.

[9] J. Kerch, A. Diez, I. Weikusat and O. Eisen, "Deriving seismic velocities on the micro-scale from c-axis orientations in ice cores," 2018.

[10] P. Cao, J. Wu, Z. Zhang, B. Fang, L. Peng, T. Li, T. J. H. Vlugt and F. Ning, "Mechanical properties of bi- and polycrystalline ice," *AIP Advances*, vol. 8, (12), pp. 125108-125108, 2018. Available: <https://www.narcis.nl/publication/RecordID/oai:tudelft.nl:uiid:feaadc8f-708b-4a18-aeba-7a9840f8e66a>.

[11] A. Maurel, J. Mercier and M. Montagnat, "Critical investigation of calculation methods for the elastic velocities in anisotropic ice polycrystals," *The Cryosphere*, vol. 10, (6), pp. 3063-3070, 2016. Available: <https://search.proquest.com/docview/1937442019>.

[12] I. Tsvankin, "Seismic Signatures and Analysis of Reflection Data in Anisotropic Media, Third edition," 2012.

[13] A. Diez and O. Eisen, "Seismic wave propagation in anisotropic ice – Part 1: Elasticity tensor and derived quantities from ice-core properties," *The Cryosphere*, vol. 9, (1), pp. 367-384, 2015. Available: <https://doaj.org/article/c0a767478d334527997f8e91c0991bd3>.

[14] S. Hellmann, M. Grab, J. Kerch, H. Löwe, A. Bauder, I. Weikusat and H. Maurer, "Acoustic velocity measurements

for detecting the crystal orientation fabrics of a temperate ice core," 2021.

[15] F. Simonetti, I. L. Satow, A. J. Brath, K. C. Wells, J. Porter, B. Hayes and K. Davis, "Cryo-Ultrasonic NDE: Ice-Cold Ultrasonic Waves for the Detection of Damage in Complex-Shaped Engineering Components," *T-Uffc*, vol. 65,

(4), pp. 638-647, 2018. Available:

<https://ieeexplore.ieee.org/document/8265626>.